Full-potential LAPW calculation of magnetic Compton profiles of Ni

Tunna Baruah, Rajendra R. Zope, and Anjali Kshirsagar*
Department of Physics, University of Pune, Pune-411007, India
(Received 9 February 2000; revised manuscript received 14 August 2000)

The full-potential linear augmented plane-wave calculation of the magnetic Compton profile is performed for Ni using both the local spin-density approximation and the generalized gradient approximation. The difference in the two results is prominent in the momentum range $0 \leq q \leq 2$ a.u. with gradient-corrected results closer to the high resolution experiment near $q=0$ along $\langle 100 \rangle$ direction. The magnetic moment is found to increase with the inclusion of the gradient correction in the exchange-correlation potential. The need for convergence of the magnetic moment with respect to the number of $\vec{k}$ points used in the calculation is stressed. The calculated magnetic Compton profiles are compared with their experimental counterparts along $\langle 100 \rangle$, $\langle 110 \rangle$, and $\langle 111 \rangle$ symmetry directions.

I. INTRODUCTION

The spin moment of nickel has received considerable attention to date as it contributes towards its ferromagnetism. Nickel has a small magnetic moment compared to other ferromagnetic $3d$ transition metals like iron. One of the experimental methods to measure the spin-moment is the magnetic Compton scattering technique. No significant orbital contribution is present in the magnetic Compton scattering under the conditions usually associated with these experiments.[1] Early measurements of the magnetic Compton profile (MCP) suffered from low statistical accuracy, which is partly due to the fact that Ni has a small magnetic moment but primarily due to the use of x-ray sources that did not have high enough intensity. The recent high energy and high intensity synchrotron sources have provided measurements of the magnetic Compton profile with a significant statistical accuracy and increased resolution,[2] ~ 0.4 a.u., compared to the earlier resolution of ~ 0.7 a.u.[3] Although the enhanced resolution of the MCP is still much lower than the resolution obtainable in the total Compton profile (~ 0.1 a.u.), a comparison of experiment and theory clearly demonstrates the usefulness of MCP studies to test the accuracy of theoretical models to describe the spin-dependent momentum density in Ni.

There have been a number of band-structure calculations of spin density of Ni resulting in calculations of the magnetic Compton profile[4–6] along with experimental measurements of MCP.[3,7] A comparison of various band-structure calculations with Fermi-surface studies and angle-resolved photoemission studies using polarized synchrotron radiation[8,9] have brought out certain discrepancies; in particular, Fermi-surface sheets due to minority bands around the X point and the exchange splitting of d bands need special mention.[10,11]

Most of the calculations are done within the local spin density approximation (LSDA) for the exchange-correlation potential. The LSDA has proved to be a reliable and tractable framework for calculating the ground-state properties of many materials but yields relatively poor results for some magnetic transition metal systems, e.g., the ferromagnetic bcc phase of Fe cannot be predicted with LSDA but is correctly ascribed with the inclusion of the generalized gradient approximation (GGA). Theory has always predicted a larger spin magnetic moment than observed experimentally, irrespective of the method of calculation. Recently Dixon *et al.*[7] reported theoretical calculations using the linear muffin-tin orbital method within the atomic-sphere approximation (LMTO-ASA) with the GGA. Although the GGA shows a tendency to enhance magnetism in transition-metal systems, different prescriptions of the GGA give considerably different results for various physical properties related to the electronic structure.[12] Thus use of a prescription of the GGA, which will improve the results over the LSDA for the properties of interest in a particular study, is essential.

Although the inclusion of the GGA has not consistently improved the band-structure or Fermi-surface (FS) results in earlier reported works, a need to include the GGA in a full-potential calculation is felt.[3,5–7] Earlier calculations, which included nonlocal effects in the exchange-correlation potential, have been performed using the LMTO-ASA.[7,13] The GGA is sensitive to the muffin-tin potential approximation in spin-polarized calculations. Moreover, the effects on the electronic wave functions and properties dependent on them have been in the right direction with the inclusion of the GGA.[13] Another important point to be noted is that all the previous calculations using the GGA employed the Perdew and Wang prescription described in Ref. 14.

Present calculations employ a prescription for the GGA as described in Ref. 15 and referred to as PW91 which is derived without semiempirical parameters and is the ''best'' functional on formal grounds.[16] It is least likely to overcorrect the subtle LSDA errors for solids. Secondly, a nonspherical spin density is used in the present calculations as deviations from sphericity of the potential are accounted for in the formalism. We feel that negative polarization of s and p electrons in ferromagnetic Ni will be considerably affected by nonlocal exchange-correlation effects which are observed at low momenta in the MCP studies. Theory overestimates the MCP near $q=0$ irrespective of the band-structure method employed for calculations and this has been attributed to electron-electron correlations inadequately treated in the LSDA. Our GGA results seem to support this fact.

In this paper we also wish to stress the importance of Brillouin-zone (BZ) sampling and the convergence of values of the magnetic moment. The need for a good $\vec{k}$ point convergence is important because the spin density seems to

 ©2000 The American Physical Society

change appreciably with the $\vec{k}$-mesh density although other quantities like band energies and total energy do not. Singh and Ashkenazi[12] have concluded that inadequate BZ sampling may lead to a spurious value of the magnetic moment as self-consistent calculations find difficulty in getting converged results for the same. Particularly, the states near the Fermi energy are important in determining the magnetic properties. Barbillieni *et al.*,[13] using the LMTO method, have tested the performance of the LSDA and the GGA in predicting various electronic-structure-related properties. Their study showed that both the LSDA and the GGA predict the same spin moment ($0.62\mu_B$) for ferromagnetic Ni. The magnetic moment calculated within the LSDA is found to be $0.596\mu_B$ using the linear combination of Gaussian orbitals[6] (LCGO) method while the full-potential linear augmented plane-wave (FPLAPW) calculations performed by Kubo and Asano[5] within the LSDA showed a value of $0.58\mu_B$, which is much closer to the experimental value of $0.56\mu_B$. The large disagreement of spin moment between the FPLAPW, LCGO, and LMTO calculations suggests that the removal of shape approximations in FPLAPW method may play an important role in this regard. Moreover, the performance of the GGA in a full-potential calculation of the MCP has not been gauged yet. It may be noted that calculations using the LCGO method or FPLAPW method have been carried out using 89 points in the 1/48 of the Brillouin zone whereas the LMTO method used a dense $\vec{k}$-point mesh.

Earlier calculations of the MCP showed a decent agreement with experiments performed with limited resolution. Most of the important structures seen in theory were lost in the convoluted curves, e.g., all the theoretical calculations showed a hump in the MCP near $q=0$ following a dip, whereas experiments reported only a central dip at $q=0$ in the $\langle 111\rangle$ direction. Recent experiments with better resolution by Dixon *et al.*[7] did support the structure predicted by theory. Their LMTO calculations also show that the GGA improves the MCP in the low momentum region where negative polarization of *s* and *p* electrons becomes important. Thus an accurate calculation of the MCP using both the full potential and the GGA is warranted to compare with the recently made available experimental data. These considerations have prompted us to undertake the present study to test the performance of the GGA and LSDA in the full-potential calculation of the magnetic Compton profile with a sufficiently large number of $\vec{k}$ points in the irreducible Brillouin zone.

The plan of the paper is as follows: Sec. II gives a brief description of the method along with the computational details while in Sec. III we discuss our results on band structure and magnetic Compton profiles in the light of recent high resolution experimental data.

II. METHODOLOGY AND COMPUTATIONAL DETAILS

The linearized augmented plane-wave (LAPW) method uses the LAPW function $\phi_{\vec{k}+\vec{G}}(\vec{r})$ as a basis to expand the all-electron wave function $\psi^j_{\vec{k}}(\vec{r})$ as follows:[17]

$$\psi^j_{\vec{k}}(\vec{r})=\sum_{\vec{G}} C^j_{\vec{k}+\vec{G}}\phi_{\vec{k}+\vec{G}}(\vec{r}), \tag{1}$$

where

$$\phi_{\vec{k}+\vec{G}}(\vec{r})=\frac{1}{\sqrt{\Omega}}\exp[i(\vec{k}+\vec{G})\cdot\vec{r}] \quad \text{for} \quad \vec{r}\in I \tag{2}$$

$$=\sum_{lm}[a^\alpha_{lm}(\vec{G})u^\alpha_l(r)+b^\alpha_{lm}(\vec{G})\dot{u}^\alpha_l(r)]Y_{lm}(\hat{\vec{r}})$$

$$\text{for} \quad \vec{r}\in S_\alpha. \tag{3}$$

Here, I and S_α denote the interstitial region and the αth muffin-tin (MT) sphere, respectively; Ω is the unit-cell volume, $a^\alpha_{lm}, b^\alpha_{lm}$, and $C^j_{\vec{k}+\vec{G}}$ are expansion coefficients, $\vec{G}$ denotes the reciprocal-lattice vector, and $u^\alpha_l(r)$ is the solution of the radial Schrödinger equation inside the αth MT sphere at the linearization energy E_l and $\dot{u}^\alpha_l(\vec{r})$ is its energy derivative. The momentum space LAPW wave function is obtained upon a Dirac-Fourier transformation of Eq. (1) as

$$A^j_{\vec{k}}(\vec{p})=\frac{1}{\sqrt{\Omega}}\int_{cell}\psi^j_{\vec{k}}(\vec{r})e^{-i\vec{p}\cdot\vec{r}}d^3r, \tag{4}$$

where $\vec{k}$ and j are the indices representing the state and band, respectively, for the electron.

The electron momentum density is computed from the momentum space wave function along with the occupancy $f^j_{\vec{k}}$, according to the equation

$$\gamma(\vec{p})=\sum_{j,\vec{k}} f^j_{\vec{k}}|A^j_{\vec{k}}(\vec{p})|^2 \tag{5}$$

from which the Compton profile is obtained by performing a double integral in a plane:[2,18,19]

$$J(p_z)=\int_{-\infty}^{\infty}\int_{-\infty}^{\infty}\gamma(\vec{p})\;dp_xdp_y. \tag{6}$$

The magnetic Compton profile along a particular direction p_z is

$$J_{mag}(p_z)=\int\int[\gamma_\uparrow(\vec{p})-\gamma_\downarrow(\vec{p})]dp_xdp_y, \tag{7}$$

where the $\gamma_{\uparrow(\downarrow)}(\vec{p})$ is the electron momentum density of the corresponding spin. The spin moment defined as

$$\mu_{spin}=\int[\gamma_\uparrow(\vec{p})-\gamma_\downarrow(\vec{p})]d\vec{p} \tag{8}$$

can be obtained from $J_{mag}(p_z)$ as

$$\mu_{spin}=\int_{-\infty}^{\infty}J_{mag}(p_z)dp_z. \tag{9}$$

A self-consistent band-structure calculation for nickel was carried out using the spin-polarized version of WIEN97.[20] The experimental lattice constant of 6.644 a.u. was used in the calculation. The exchange-correlation potentials parametrized by Perdew and Zunger[21] from the data of Ceperley and Alder[22] (CA) and that of von Barth and Hedin[23] (VBH) were used for the LSDA while for calculations using the

TABLE I. The magnetic moments of Ni within different exchange-correlation formalisms.

Number of $\vec{k}$ points	VBH μ_B	CA μ_B	PW91 μ_B	PBE μ_B
72	0.580	0.588	0.603	0.612
286	0.598	0.609	0.624	0.633
560	0.602	0.612	0.626	0.635

GGA, the form given by Perdew and Wang[15] (PW91) and also its simplified version[24] (PBE) were employed. The self-consistent band structure was obtained using 560 $\vec{k}$ points in 1/48th of the Brillouin zone. 916 $\vec{k}$ points in 1/48th Brillouin zone yielding 916×2109 $\vec{p}$ points were used for the calculation of the magnetic Compton profiles. The tetrahedron integration scheme of Lehman and Taut[25] was employed for the integrations in the reciprocal space. The spin-polarized core Compton profiles were calculated with a highly accurate version of the density-functional-based Herman-Skillman[26] program.

III. RESULTS AND DISCUSSION

The spin contribution to the magnetic moment of nickel has experimentally been determined to be $0.56\mu_B$. We present the values of the spin moment obtained from our band-structure calculation using different LSDA and GGA exchange-correlation potentials in Table I. From the table it is obvious that the choice of the exchange-correlation potential plays an important role in determining the spin moment, the GGA worsening the comparison with the experimental value. The different values are a result of different potentials that result under various parametrizations of the exchange-correlation potential. The magnetic moment value, being an integral over the entire space of the spin density, is very sensitive to these differences. Another point to be noted is that the difference between the magnetic moments calculated within two different parametrizations of the LSDA (CA and VBH) and the GGA (PW91 and PBE) turns out to be of the same order as the difference of this quantity calculated within the LSDA and the GGA. Since PBE functional is essentially a simplification of the PW91 functional, it seems that the magnetic moment is very sensitive to the nature of the exchange-correlation potential and going beyond the LSDA does not prove to be effective for determination of its value. It is to be noted that the LSDA models the exchange-correlation hole around an average electron rather than yielding accurate results for all positions of the electron and also that the GGA favors inhomogeneity in the electron density more than the LSDA does.

A point that needs to be emphasized here is that the number of $\vec{k}$ points used to obtain the self-consistent spin-polarized band structure is an important factor in deciding the value of the spin moment. In our calculations, it was observed that spin moment increases as the $\vec{k}$ mesh is refined, convergence being achieved with ~ 500 $\vec{k}$ points in 1/48th part of the Brillouin zone. This point was stressed by Singh and Ashkenazi[12] in the context of the FPLAPW calculation of magnetism in Cr, V, and Pd. Our calculations bring out the fact that employing ~ 100 $\vec{k}$ points in the irreducible Brillouin zone may be sufficient for convergence of band energies and total energy but is certainly not adequate for wave-function-dependent properties like charge density, momentum density, etc. In the following we present our results using the VBH prescription for the LSDA and PW91 for the GGA to bring out the effect of inclusion of nonlocal effects in the exchange-correlation potential.

TABLE II. Comparison of the Fermi-surface breaks of the majority bands in units of $2\pi/a$ along symmetry directions.

Direction	FPLAPW		Ref. 13		Expt.
	VBH	PW91	LSDA	GGA	Refs. 31 and 32
Γ-X	0.77	0.77	0.77	0.77	0.77
Γ-K	0.59	0.60	0.59	0.60	0.58
K-W	0.05	0.05	0.05	0.04	0.05

In order to study the effect of the gradient corrected exchange-correlation potential on the spin momentum density, we first discuss its effect on the spin-polarized band structure. The band structure and Fermi surface for majority spin are not affected by inclusion of gradient corrections (see Table II).

A major point of discrepancy between theoretically and experimentally observed band structures of Ni has been the hole pockets around the X point due to the minority bands. Such a hole pocket for $X_{2\downarrow}$ was predicted by all earlier theoretical calculations, irrespective of the method employed and the form of the exchange-correlation potential used. But de Haas–van Alphen effect measurements[27] concluded that $X_{2\downarrow}$ is below the Fermi energy (E_F). Also, the measurements for the hole pocket due to $X_{5\downarrow}$ did not agree with theory. Some evidence to the contrary, from studies on angular variation of magnetic anisotropy, predicting that $X_{2\downarrow}$ will almost be at E_F, also exists.[28] This disagreement between experiment and theory has been ascribed to the LSDA, particularly to the neglect of density gradient terms. An inhomogeneity correction involving second-order terms in $\vec{\nabla}\rho(\vec{r})$ is expected to push $X_{5\downarrow}$ (t_{2g} symmetry) and $X_{2\downarrow}$ (e_g) apart so that the latter is below E_F. Thus different splittings of t_{2g} and e_g that are not resolved in the LSDA might show up in the GGA. Spin-polarized band structure using the LSDA with inclusion of spin-orbit (SO) coupling by Wang and Callaway[29] also did not alter the band structure much, except for lifting accidental degeneracies; the Fermi surface was not affected. The mixing of up and down contributions with SO coupling may introduce changes in magnetic properties, thus affecting the value of the magneton number.[29] Our calcula-

TABLE III. Comparison of the Fermi-surface breaks of the minority bands in units of $2\pi/a$ along symmetry directions.

Direction	FPLAPW		Ref. 29	Expt.	
	VBH	PW91	LSDA	Ref. 32	Ref. 27
X-Γ	0.228	0.224	0.206	0.220	0.219
X-W	0.134	0.100	0.081	0.112	0.105
Γ-L	0.168	0.168			

tions with the GGA show the existence of a hole pocket corresponding to $X_{2\downarrow}$ though it is small. The eigenvalues of the minority X_2 band are 0.008 Rydberg within the LSDA and 0.003 Rydberg within the GGA with respect to the E_F. The correction due to the GGA is in the right direction, although small. On the other hand, the value of $X_{5\downarrow}$ within the GGA is raised above the LSDA value. Our calculated value of the $X_{5\downarrow}$ within the LSDA is higher than the values of Wang and Callaway[30] using the LCGO with the LSDA. Callaway and Wang[10] have attributed the higher value of the $X_{2\downarrow}$ hole pocket and the lower value of the $X_{5\downarrow}$ hole pocket to the noninclusion of the nonspherical terms in the effective potential. In this regard, our full-potential calculation within the LSDA improves the hole pocket associated with the $X_{5\downarrow}$ band while the one associated with the $X_{2\downarrow}$ band remains same. The GGA indeed lifts the $X_{5\downarrow}$ band up and brings the $X_{2\downarrow}$ band down. However, with the GGA the spurious hole pocket is not completely eliminated (see Table III).

Another point of discrepancy between the theoretical and experimental measurements has been the magnitude of exchange splitting in ferromagnetic nickel. The values of the exchange splitting throughout the *d* band determined by the photoemission experiments have differed from theoretical calculations roughly by a factor of 2. A similar trend is seen in the present calculation. This disagreement is assigned to the limitations of the one-electron picture used in all calculations.

A comparison of the scalar-relativistic calculation of the position space-charge density with nonrelativistic results shows the charge density near sphere centers to be significantly different. Therefore, a scalar-relativistic calculation is performed. The nonlocal effects due to the inclusion of the gradient correction in the exchange-correlation potential will be observable at low momentum values in the MCP or spin momentum density.

The calculated magnetic Compton profiles along three symmetry directions $\langle 100\rangle$, $\langle 110\rangle$, and $\langle 111\rangle$ obtained using both the LSDA and GGA are presented in Fig. 1. The experimental values are those obtained by Dixon *et al.*[7] The theoretical MCP's are convoluted with the experimental resolution function. Our theoretical profiles were renormalized to the value of the magnetic moment calculated by the band-structure method to facilitate a direct comparison with the experimental results which were renormalized to the known magnetic moment within a given region.[7] The various structures unveiled in the MCP are a consequence of the Fermi-surface topology and anisotropy in the electron momentum distribution. Structures observed up to $q=1$ a.u. come from the first Brillouin zone which again appear in the higher zones as umklapp images. The umklapp images are more prominently visible in the $\langle 110\rangle$ direction and also to a lesser extent in the $\langle 100\rangle$ direction. Bands 1 to 4 contribute little to the total magnetic moment as these bands are almost filled for minority and majority spins. Near $q=0$, negative polarization due to the *s*- and *p*-like bands is clearly visible. However, it is the fifth band which is occupied for the majority spin and becomes partly unoccupied for the minority spin. Thus the structures seen in the total MCP predominantly come from the fifth band. The sixth band has a significant contribution towards the magnetic moment and is responsible for valleylike structures seen in the low-q region.

A comparison of the present results with earlier published results reveals the following trends: the present values of the MCP are higher than the values reported by Kubo and Asano[5] in the region $q<2$ a.u. in all three symmetry directions. This is a manifestation of the number of $\vec{k}$ points used for the band-structure calculations. The nature of the contribution from the third and fourth band changes with the number of $\vec{k}$ points in all three directions although their contribution to the magnetic moment is small. Calculations with the LMTO method overestimate the MCP everywhere and the structures up to 2 a.u. are exaggerated. This may be attributed to the effect of the shape approximation to the potential inherent in the LMTO-ASA. The GGA enhances all the structures in the total MCP in comparison to the LSDA. This is displayed in the present study as well as in the work of Dixon *et al.*[7] (see Tables II and III). Although the GGA enhances the negative polarization of *s*- and *p*-like bands, the positive enhancement from the fifth and sixth bands is also more, resulting in a higher value for the magnetic moment for the GGA in comparison to the LSDA. The negatively polarized contribution from the interstitial electrons is $-0.043\mu_B$ and $-0.031\mu_B$ within the GGA and LSDA, respectively. In the high momentum region, both the GGA and LSDA values match the experimental ones more or less. However, due to the low resolution of the experimental setup, the structures seen in the theoretical profiles are not distinctly discernible in the experimental profiles. The structures seen in the theoretical profiles in the high momentum region are smeared out due to convolution with the experimental resolution function. Most importantly, our full-potential GGA calculations improve the agreement with experiment near $q=0$ along the $\langle 100\rangle$ direction. In the following we discuss some salient observations for MCP along particular directions.

In the profile along the $\langle 100\rangle$ direction (Fig. 1, first panel), the depth of the dip around $q=0$ is reproduced in our calculation with the GGA but with the LSDA it is higher than the experimental value. A comparison with Fig. 3 given by Dixon *et al.*[7] shows that the LMTO-GGA profile is slightly higher than the experimental value near $q=0$; the LMTO-LSDA shows an extra peak below 1 a.u. whereas the LMTO-GGA reveals a shoulderlike structure. Our calculations reveal a broad shoulder near this q value. The nonlocal corrections included in the GGA therefore improve the profile at and around $q=0$. However, in the region $q\sim 2.0$ a.u., the theoretical profiles are overestimated. Although the GGA improves the profile below ~ 1 a.u., beyond 1 a.u. the GGA values are higher than the LSDA values. In the region 1 a.u. $<q<2$ a.u., which corresponds to the second Brillouin zone, there is another shoulderlike structure seen around ~ 1.3 a.u. in all the theoretical profiles which is not observed in the experimental ones. This observation warrants experiments with better resolution. This structure is the umklapp image of the shoulder near $q=0.6$ a.u. The values of the theoretical profiles are much higher than experimental ones, justifying the higher spin moment found in theoretical calculations. The bandwise contributions in the $\langle 100\rangle$, $\langle 110\rangle$, and $\langle 111\rangle$ directions within both the LSDA and the GGA are shown in Figs. 2, 3, and 4, respectively, for any future comparison. These profiles are

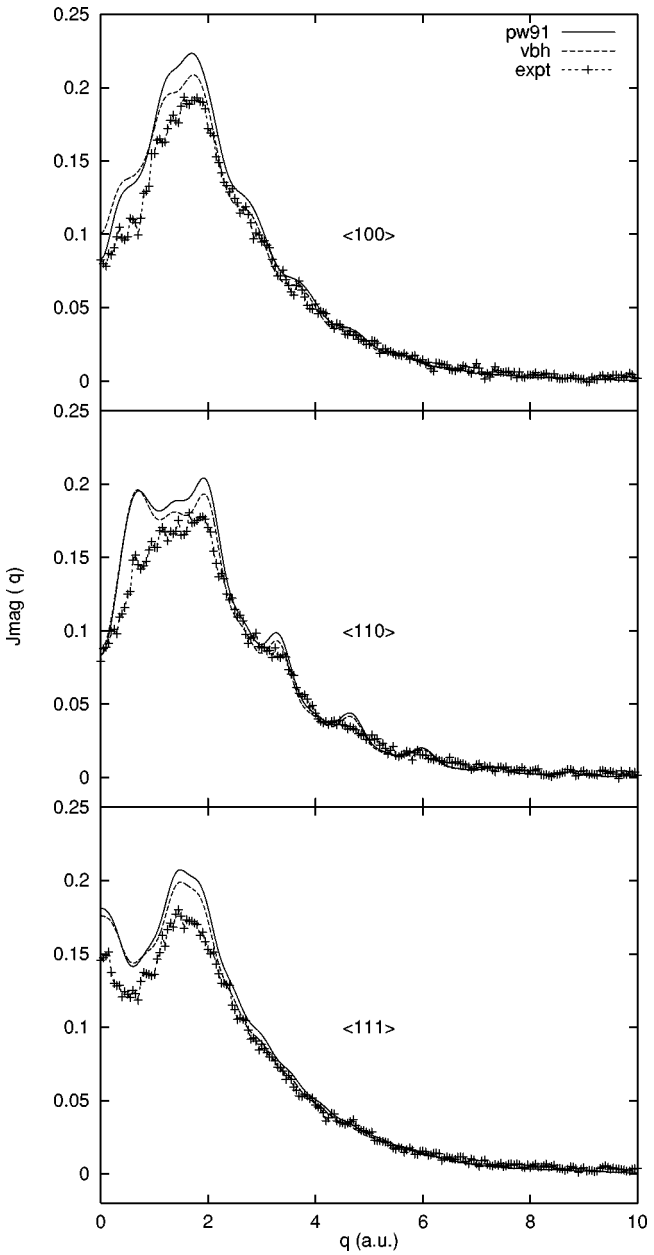

FIG. 1. Magnetic Compton profiles of Ni along ⟨100⟩, ⟨110⟩, and ⟨111⟩ directions.

not convoluted. The contribution from core electrons towards the magnetic Compton profile, which is small and does not have much structure, is not shown.

In the ⟨110⟩ direction, an extra prominent peak is seen in the theoretical magnetic Compton profiles (Fig. 1, second panel) within both the GGA and the LSDA at around ~ 0.7 a.u., which is not clearly visible in the experimental profile, again probably due to low resolution. It may be mentioned here that the LMTO method displays the most prominent peak at 0.7 a.u. whose value is reduced on the inclusion of gradient correction. The FPLAPW method within the GGA displays this peak to be lower in value than the peak at ~ 2 a.u. The values near $q=0$ are well reproduced within both the LSDA and GGA in this direction also. In this case, the LSDA profile lies closer to the experimental values in the region $1<q<2$ a.u. Although the values of the theoretical profiles are higher than the experimental ones in this region,

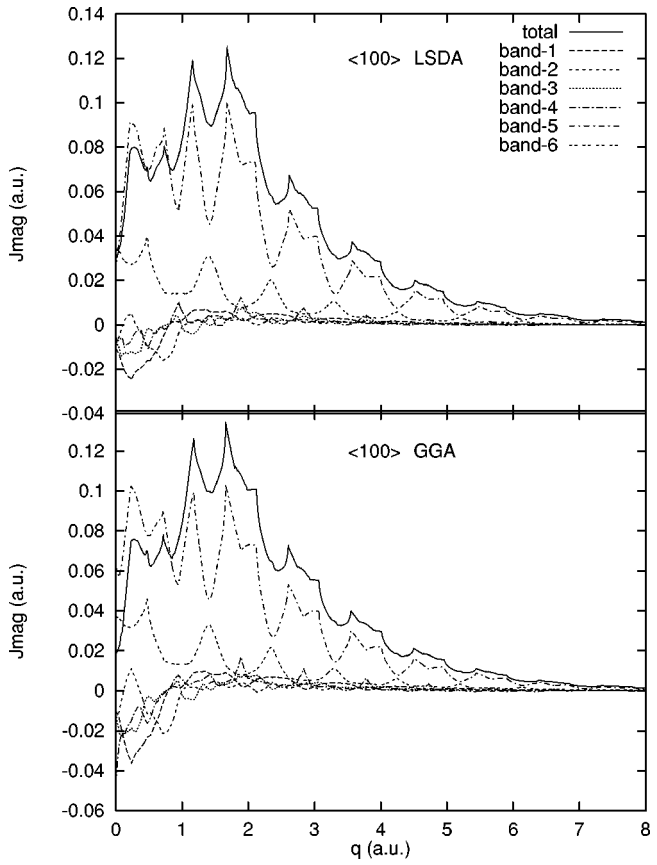

FIG. 2. Bandwise magnetic Compton profiles of Ni along the ⟨100⟩ direction within both the LSDA and the GGA.

the structures are well reproduced. The high momentum components are more prominent in the theoretical profiles than in the experimental one. However, GGA results show periodic structures due to umklapp images more pronounced than LSDA results.

In Fig. 3 the negative polarization of the *s*- and *p*-like bands can be seen distinctly. This negative polarization produces the dip in the MCP in the low-q region. Although the contributions from the fifth and the sixth bands have almost the same structure within both the LSDA and the GGA, the contributions of the lower bands, especially the negative polarization, are different within the two approximations. Moreover, the structure of the peak ~ 0.7 a.u. is decidedly different within both the LSDA and the GGA.

Although the FPLAPW method with GGA produces good agreement with experimental profiles near the $q=0$ momentum region in both ⟨100⟩ and ⟨110⟩ directions, in the ⟨111⟩ direction the improvement is minimum with the theoretical profile lying much above the experimental one (Fig. 1, third panel). In this direction, the agreement of the results of Kubo and Asano[5] is much better than ours. However, this may be due to the smaller spin moment obtained by them. The LMTO results of Dixon *et al.*[7] also show an overestimated profile. It is gratifying to see that all the structures in the experimental MCP are well reproduced by theory in this direction at the correct q values. It should be noted here that earlier experiments showed only a central dip near $q=0$ in this direction whereas all theoretical calculations predicted a small peak at $q=0$ and a dip around 0.7 a.u. Better resolution available in the work of Dixon *et al.*[7] has brought out

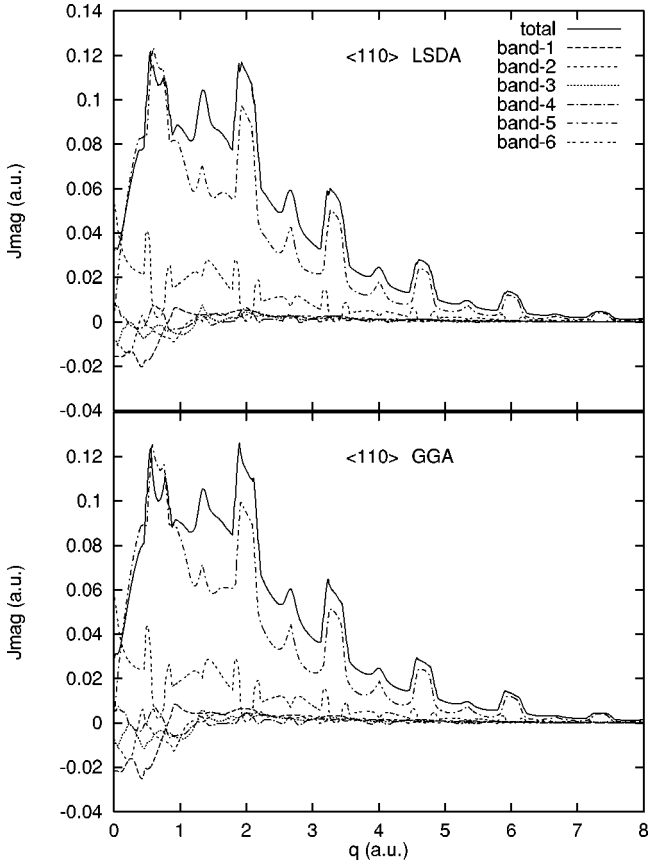

FIG. 3. Bandwise magnetic Compton profiles of Ni along the ⟨110⟩ direction within both the LSDA and the GGA.

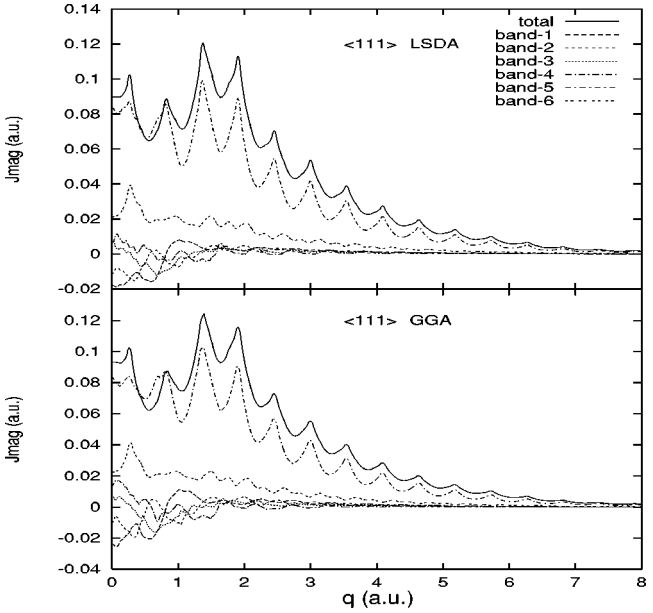

FIG. 4. Bandwise magnetic Compton profiles of Ni along the ⟨111⟩ direction within both the LSDA and the GGA.

the structure predicted by theory. Experiment and theory match quite well beyond 4 a.u. and the results within the GGA and the LSDA are also same. Figure 4 reveals that there is a redistribution of the spin density among the various bands amounting even to changes in the structure in going from the LSDA to the GGA. The overall structure of the total MCP is, however, not changed drastically. Thus, it is apparent that the GGA affects the MCP's of Ni in the momentum region $0 \leqslant q \leqslant 2$ a.u.

As pointed out earlier, the MCP depends on the Fermi-surface topology and the electron momentum density of majority and minority bands. The inclusion of spin-orbit coupling in the calculations will affect the crossing of the bands at E_F due to hybridization of up and down densities. This in turn will affect the peak values seen in the MCP curves as they are the images of the FS breaks. Another source of discrepancy for a finer comparison of theory with experiment is the so-called Lam-Platzman (LP) correction.[33] The calculations using density-functional theory are carried out within Kohn-Sham noninteracting picture. The electron momentum density calculated from the single-particle orbitals has to be augmented by a correction term. Although this correction as proposed[33] is exact, it cannot be evaluated exactly. Model calculations to extract the correction numerically[34,35] employ an isotropic momentum density. Since the spin momentum density in Ni is highly anisotropic, LP corrections, as routinely incorporated in the total CP calculations, have not been included in the present work.

In conclusion, the spin density of ferromagnetic nickel was studied within both the generalized gradient and local spin-density approximations using full-potential calculations. The convergence of the spin density with respect to the number of $\vec{k}$ points in the irreducible Brillouin zone was ensured. The effect of the GGA is visible in the band structure as well as in the spin momentum density. The GGA reduces some discrepancies of the LSDA results with experiments like the spurious $X_{2\downarrow}$ hole pocket but does not completely eliminate it. On the other hand, the exchange splittings, which are already overestimated in the LSDA, increase with the inclusion of the nonlocal effects. This supports the fact that the GGA enhances magnetism of *d* electrons. The magnetic Compton profiles with no shape approximation to the potential show better agreement with the experimental values and the gradient correction to the exchange-correlation potential improves results along the ⟨100⟩ direction. The GGA is found to be important for the structures in the MCP near $q = 0$ although it overestimates the magnetic moment. The magnetic moment is found to be sensitive to the form of the exchange-correlation potential as well as the Brillouin-zone sampling.

ACKNOWLEDGMENTS

We gratefully acknowledge the experimental data provided by Dr. J. Duffy and Professor M. J. Cooper and his group. We are grateful to Professor K. Schwarz and Dr. P. Blaha for providing the WIEN97 code. T.B. and R.R.Z. gratefully acknowledge the financial support from the Council for Scientific and Industrial Research, New Delhi. A.K. acknowledges financial support from University Grants Commission, New Delhi.

*Author to whom all correspondence should be addressed.
[1] M. J. Cooper, E. Zukowski, S. P. Collins, D. N. Timms, F. Itoh, and H. Sakurai, J. Phys.: Condens. Matter **4**, L399 (1992).
[2] M. J. Cooper, Radiat. Phys. Chem. **50**, 63 (1997).
[3] N. Sakai, M. Ito, H. Kawata, T. Iwazumi, M. Ando, N. Shiotani, F. Itoh, Y. Sakurai, and S. Nanao, Nucl. Instrum. Methods Phys. Res. A **303**, 488 (1991).
[4] P. Rennert, G. Carl, and W. Hergert, Phys. Status Solidi B **120**, 273 (1983).
[5] Y. Kubo and S. Asano, Phys. Rev. B **42**, 4431 (1990).
[6] V. Sundararajan and D. G. Kanhere, J. Phys.: Condens. Matter **3**, 3311 (1991).
[7] M. A. G. Dixon, J. A. Duffy, S. Gardelis, J. E. McCarthy, M. J. Cooper, S. B. Dugdale T. Jarlborg, and D. N. Timms, J. Phys.: Condens. Matter **10**, 2759 (1998).
[8] W. Eberhardt and E. W. Plummer, Phys. Rev. B **21**, 3245 (1980).
[9] F. J. Himpsel, J. A. Knapp, and D. E. Eastman, Phys. Rev. B **19**, 2919 (1979).
[10] J. Callaway and C. S. Wang, Physica B **91**, 337 (1976).
[11] R. Ahuja, S. Auluck, and B. Johansson, Phys. Scr. **50**, 573 (1994).
[12] D. J. Singh and J. Ashkenazi, Phys. Rev. B **46**, 11 570 (1992).
[13] B. Barbillieni, E. G. Moroni, and T. Jarlborg, J. Phys.: Condens. Matter **2**, 7597 (1990).
[14] J. P. Perdew, Phys. Rev. Lett. **55**, 1665 (1985); J. P. Perdew and Y. Wang, Phys. Rev. B **33**, 8800 (1986); J. P. Perdew, *ibid.* **33**, 8822 (1986).
[15] J. P. Perdew and Y. Wang, Phys. Rev. B **45**, 13 244 (1992); J. P. Perdew, in *Electronic Structure of Solids '91*, edited by P. Ziesche and H. Eschrig (Akademic Verlag, Berlin, 1991), p. 11.
[16] K. Burke and J. P. Perdew, Int. J. Quantum Chem. **56**, 199 (1995).
[17] D. Singh, *Planewaves, Pseudopotentials and the LAPW Method*, (Kluwer Academic, Boston, 1994).
[18] J. Rath, C. S. Wang, R. A. Tawil, and J. Callaway, Phys. Rev. B **8**, 5139 (1973).
[19] C. T. Venkataraman, J. C. Lang, C. S. Nelson, G. Srajer, D. R. Haeffner, and S. D. Shastri, Rev. Sci. Instrum. **69**, 1970 (1998).
[20] P. Blaha, K. Schwarz, and J. Luitz, WIEN97, Vienna University of Technology, 1997. [Improved and updated Unix version of the original copyrighted WIEN code, which was published by P. Blaha, K. Schwarz, P. Sorantin, and S. B. Trickey, Comput. Phys. Commun. **59**, 399 (1990)].
[21] J. P. Perdew and A. Zunger, Phys. Rev. B **23**, 5048 (1981).
[22] D. M. Ceperley and B. J. Alder, Phys. Rev. Lett. **45**, 566 (1980).
[23] U. von Barth and L. Hedin, J. Phys. C **5**, 1629 (1972); A. K. Rajagopal, *Advances in Chemistry and Physics*, edited by G. I. Prigogine and S. A. Rice (Wiley, New York, 1979), Vol. 41.
[24] J. P. Perdew, K. Burke, and M. Ernzerhof, Phys. Rev. Lett. **77**, 3865 (1996).
[25] G. Lehman and M. Taut, Phys. Status Solidi B **54**, 469 (1974).
[26] F. Herman and S. Skillman, *Atomic Structure Calculation* (Prentice-Hall, New Jersey, 1963).
[27] D. C. Tsui, Phys. Rev. **164**, 669 (1967).
[28] R. Gersdorf, Phys. Rev. Lett. **40**, 344 (1978).
[29] C. S. Wang and J. Callaway, Phys. Rev. B **9**, 4897 (1974).
[30] C. S. Wang and J. Callaway, Phys. Rev. B **15**, 298 (1977).
[31] D. C. Tsui and R. W. Stark, Phys. Rev. Lett. **19**, 655 (1967).
[32] L. Hodges, D. R. Stone, and A. V. Gold, Phys. Rev. Lett. **19**, 655 (1967).
[33] L. Lam and P. M. Platzman, Phys. Rev. B **9**, 5122 (1974); **9**, 5128 (1974).
[34] B. Y. Tong and L. Lam, Phys. Rev. A **18**, 5128 (1978).
[35] D. A. Cardwell and M. J. Cooper, J. Phys.: Condens. Matter **1**, 9357 (1989).